Contribution from the Departments of Chemistry and Physics, Washington State University, Pullman, Washington 99164, Departmento di Chemica, Università di Modena, 41100 Modena, Italy, and Instituto di Chemica Generali e Inorganica dell'Università di Parma, Centro di Studio per la Strutturistica Diffrattometrica del CNR, 43100 Parma, Italy

Structures and Magnetic Properties of Trinuclear Copper(II) Halide Salts

Todd E. Grigereit,[1a,b] B. L. Ramakrishna,[1a,c] Helen Place,[1a] Roger D. Willett,*[1a] Gian Carlo Pellacani,[1d] Tiziano Manfredini,[1d] Ledi Menabue,[1d] Anna Bonamartini-Corradi,[1e] and Luigi Pietro Battaglia[1e]

Received December 22, 1986

The crystal structures of a series of trinuclear copper(II) halide salts have been determined. These all contain pseudoplanar, symmetrically bibridged $Cu_3X_8^{2-}$ (Ia) or $Cu_3X_7L^-$ (Ib) anions. ACu_3Cl_8 or $A_2Cu_3Cl_8$ salts are formed with A being the

Ia Ib

N-methylpiperazinium (NMPZ), 3-methyl-2-aminopyridinium (3MAP), and 5-methyl-2-aminopyridinium (5MAP) cations. A $Cu_3Br_8^{3-}$ analogue is found with the 5-bromo-6-methyl-2-aminopyridinium (5B6MAP) cation. With the methylphenethylammonium (NMPH) cation, a (NMPH)Cu_3Cl_7·EtOH salt is isolated. The salts are all monoclinic with the following space group and lattice constants: NMPZ, $C_5H_{14}N_2Cu_3Cl_8$, $P2_1/c$, a = 6.840 (3) Å, b = 14.321 (9) Å, c = 9.890 (5) Å, β = 102.90 (5)°, Z = 4; 3MAP, $C_{12}H_{18}N_4Cu_3Cl_8$, $C2/c$, a = 26.05 (1) Å, b = 13.687 (4) Å, c = 7.099 (3) Å, β = 117.95 (3)°, Z = 4; NMPH, $C_{11}H_{20}NOC_3Cl_7$, $P2_1/n$, a = 11.843 (4) Å, b = 7.626 (3) Å, c = 23.840 (10) Å, β = 79.61 (3)°, Z = 4; 5B6MAP, $C_{12}N_{10}N_4$-Cu_3Br_{10}, $P2_1/n$, a = 13.216 (3) Å, b = 4.076 (1) Å, c = 24.614 (6) Å, β = 91.65 (2)°, Z = 2. Each copper ion extends its primary coordination by formation of two semicoordinate bonds to halide ions in adjacent oligomers, yielding the familiar 4+2 coordination geometry for copper(II) complexes. These additional linkages cause the oligomers to aggregate into stacks, yielding stacking patterns of type IIa (NMPZ, 3MAP salts) or type IIb (NMPH, 5MAP, and 5B6MAP). Cu–X distances are approximately 2.3

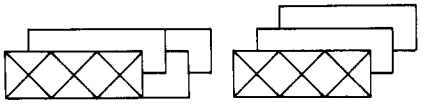

IIa IIb

Å (Cl) or 2.4 Å (Br) within the oligomers and 2.7–3.3 Å (Cl) or 3.2–3.3 Å (Br) between oligomers. The bridging Cu–X–Cu angles within the trimer average near 94°. Magnetic susceptibility measurements have been made on the NMPZ, NMPH, 3MAP, and 5MAP chloride salts. In addition, measurements were performed on $Cu_3Cl_6(CH_3CN)_2$, which contains neutral trinuclear oligomers. All compounds have doublet ground states arising from antiferromagnetic exchange coupling between neighboring copper(II) ions. The value of J/k is typically −20 to −35 K, consistent with the structural characteristics of the trimeric species.

Introduction

The stereochemistry of copper(II) complexes is exceedingly rich and diverse.[2] The copper(II) ion exhibits two types of coordination to ligands: normal coordination, with an ionic radius of approximately 0.50 Å, and a semicoordination in which the bond lengths are typically 0.3–1.0 Å longer than those with normal coordination. Coordination numbers range from 4 to 6, but coordination geometries are rarely regular.[3] They include geometries that are four-coordinate, ranging from square planar to distorted tetrahedral,[4] five-coordinate, with variation among square-pyramidal, trigonal-bipyramidal, and 4+1 geometries,[5] and six-coordinate, with a 4+2 geometry.[6]

The diversity in coordination geometry is particularly evident in copper(II) halide salts, since the halide ions impose little stereochemical restriction. Thus, the observed geometries represent a delicate balancing of crystal field stabilization energies, halide ion–halide ion electrostatic repulsive energies, hydrogen bonding, and the ever-ubiquitous crystal-packing energies. This frequently leads to the situation where two or more different geometries coexist within the same structure.[7] In addition, the halide ions are able to function as bridging ligands, leading to the formation of oligomers and extended structures.[8,9] This allows for the possibility of a bewildering array of structural types. We have recently reviewed the structural chemistry of $ACuCl_3$ salts,[8] but since that time two new structural types have been reported.[10,11] The structures of copper(II) halide salts have been of particular interest in an attempt to understand the correlations between structural parameters and magnetic properties in inorganic systems.[12]

One particularly common polynuclear structural type is the pseudoplanar bibridged $Cu_nX_{2n}L_2$ oligomer, where X = Cl^-, Br^- and L = monodentate ligand (including Cl^- or Br^-, as well as neutral ligands) with $n \leq 5$.[9] These are sections of the infinite chains present in anhydrous $CuCl_2$ and $CuBr_2$[13] (III). Each

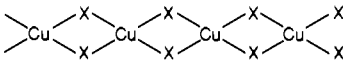

III

copper(II) ion assumes a primary square-planar configuration. In the CuX_2 salts, adjacent chains are displaced (stacked) so that the copper(II) ions form semicoordinate Cu–X bonds to halide

* To whom correspondence should be addressed.

(1) (a) Department of Chemistry, Washington State University. (b) Department of Physics, Washington State University. (c) Present address: Department of Chemistry, Arizona State University, Tempe, AZ. (d) Università di Modena. (e) Centro di Studio per la Strutturistica Diffrattometrica del CNR.
(2) Smith, D. W. *Coord. Chem. Rev.* **1976**, *21*, 92 and references therein.
(3) Hathaway, B. *Coord. Chem. Rev.* **1982**, *41*, 423 and references therein.
(4) Harlow, R. L.; Wells, W. J.; Watt, G. W., III; Simonsen, S. H. *Inorg. Chem.* **1975**, *14*, 1786. Battaglia, L. P.; Bonamartini-Corradi, A.; Marcotrigiano, G.; Menabue, L.; Pellacani, G. C. *Inorg. Chem.* **1979**, *18*, 2106.
(5) Antolini, L.; Marcotrigiano, G.; Menabue, L.; Pellacani, G. C. *J. Am. Chem. Soc.* **1980**, *102*, 1303. Gill, N. S.; Sterns, M. *Inorg. Chem.* **1970**, *9*, 1619. Vaciago, A.; Zambonelli, L. *J. Chem. Soc. A* **1970**, 218.
(6) Dubler, E.; Korber, P.; Oswald, H. R. *Acta Crystallogr., Sect. B: Struct. Crystallogr. Cryst. Chem.* **1973**, *B29*, 1929. Distler, T.; Vaughan, P. A. *Inorg. Chem.* **1967**, *6*, 126.
(7) Antolini, L.; Marcotrigiano, G.; Menabue, L.; Pellacani, G. C. *J. Am. Chem. Soc.* **1980**, *102*, 5506. Clay, R. M.; Murray-Rust, P.; Murray-Rust, J. *J. Chem. Soc.* **1973**, 595.
(8) Geiser, U.; Willett, R. D. *Croat. Chem. Acta* **1984**, *57*, 737.
(9) Geiser, U.; Willett, R. D.; Lindbeck, M.; Emerson, K. *J. Am. Chem. Soc.* **1986**, *108*, 1173.
(10) Honda, M.; Katayama, C.; Tanaka, J.; Tanaka, M. *Acta Crystallogr., Sect. C: Cryst. Struct. Commun.* **1985**, *C41*, 197, 688.
(11) Geiser, U.; Willett, R. D. *Inorg. Chem.* **1986**, *25*, 4203.
(12) Willett, R. D. *NATO ASI Ser., Ser. C* **1985**, *No. 140*, 389. Hatfield, W. E. *Ibid.* **1985**, *No. 140*, 555.
(13) Wells, A. F. *J. Chem. Soc.* **1947**, 1670. Helmholz, L.; Kruh, R. F. *J. Am. Chem. Soc.* **1952**, *74*, 1176.

0020-1669/87/1326-2235$01.50/0

ions in neighboring chains. This yields a 4+2 coordination geometry. For the finite oligomers, variations in their stacking occur, yielding the possibility of either 4+1 or 4+2 coordination. We have developed a graphical representation, as well as a shorthand notation, to specify a given stacking arrangement. These are exemplified by the patterns for $KCuCl_3$[14] (IVa), $[(CH_3)_2CHNH_2]CuCl_3$[15] (IVb), and $(melH_2)Cu_2Cl_6$[16] (IVc, $melH_2$ = melaminium). The graphical representation simply consists of an illustration of the stacking of "envelopes", where each envelope represents the pseudoplanar oligomer. The stacking of the envelopes shows the manner in which adjacent oligomers are translated so as to form the semicoordinate bonds between oligomers. The shorthand notation is of the form $n(d_{\parallel},d_{\perp})$. Here n is the number of copper(II) ions in the oligomer. The relative in-plane displacements between adjacent oligomers, $d_{\parallel}$ and $d_{\perp}$, are specified in terms of units of the X–X distances on the edge of the oligomers. As many displacement symbols as necessary are concatonated. In $KCuCl_3$ (IVa) the $2(^1/_2,^1/_2)$ pattern is a simple segment out of the $CuCl_2$ structure, such that each copper(II) ion has a 4+2 coordination. The $2(^1/_2,^3/_2)$ pattern, as for the dimers in $[(CH_3)_2CHNH_3]CuCl_3$ (IVb) again is a segment of the $CuCl_2$ structure. However, the copper(II) ions in each oligomer only attain a 4+1 coordination through the stacking. Finally, the more complex $2(^1/_2,^1/_2)(^1/_2,^{-1}/_2)$ pattern in IVc retains the 4+2 coordination but now can no longer be viewed as derived from the CuX_2 structures.

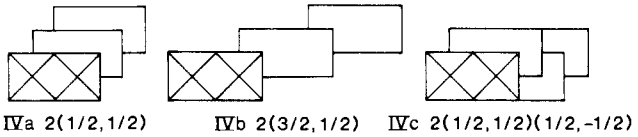

IVa 2(1/2,1/2) IVb 2(3/2,1/2) IVc 2(1/2,1/2)(1/2,-1/2)

In this paper, we report the structures and magnetic properties of a series of trinuclear copper(II) oligomers. Previously reported pseudoplanar bibridged halide trimers include those found in $Cu_3Cl_6(CH_3CN)_2$,[17] $Cu_3Cl_6(H_2O)_2{\cdot}2(CH_2)_4SO_2$,[18] and $[(C_2H_5)_2NH_2]_2(Cu_3Br_8){\cdot}CuBr_2{\cdot}EtOH$[9] with stacking patterns Va, Vb, and Vc, respectively. A $Cu_3Cl_{14}^{8-}$ trimer is found in $(C_6N_3H_{18})_4Cu_5Cl_{22}$.[7a] A variety of other trinuclear species have been observed including such diverse systems as bis(adeninium) octachlorotricuprate(II) tetrahydrate,[20] $Cu_3(N\text{-nico})_4(OH)_2(H_2O)_2$, where N-nico is nicotinate N-oxide,[21] $Cu_3L_2(CH_3COO)_4$, where LH = N-methyl-N'-(4-methoxysalicylidene)-1,3-propanediamine,[22] and numerous other Schiff base complexes.[23-27] Magnetic studies have been carried out on many of these systems.[18-20,22-27] The compounds reported in this paper were synthesized as part of our program to correlate the structural and magnetic properties in copper(II) halides.

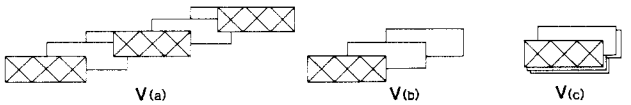

V(a) V(b) V(c)

Preparation

The general procedure for preparation of the chloride salts involved reaction of the amine hydrochloride with excess anhydrous copper(II) chloride in an alcoholic or acid solvent. In general, n-propanol was the solvent of choice, although methanol or ethanol could be substituted. Crystalline materials were obtained by slow evaporation of the alcoholic solutions. For the bromide salt, aqueous solutions were utilized to minimize reduction to copper(I).

Bis(3-methyl-2-aminopyridinium) Octachlorotricuprate(II) ($(3MAP)_2Cu_3Cl_8$, $C_{12}H_{18}N_4Cu_3Cl_8$). The free amine, 3-methyl-2-aminopyridine, was monoprotonated by titration with a dilute HCl solution. The pyridinium chloride salt was isolated and reacted with stoichiometric quantities of anhydrous $CuCl_2$ in ethanol to yield $(3MAP)CuCl_3$. These reddish brown platelets were redissolved in n-propanol with excess $CuCl_2$. Evaporation of the resultant solution yielded fine orange-brown needles of $(3MAP)_2Cu_3Cl_8$. Anal. Found (calcd): C, 20.50 (20.81); H, 4.01 (2.62); N, 7.97 (8.09); Cl, 40.34 (40.95).

Bis(5-methyl-2-aminopyridinium) Octachlorotricuprate(II) ($(5MAP)_2Cu_3Cl_8$, $C_{12}H_{18}N_2Cu_3Cl_8$). This was prepared as above except that the isolation of the intermediate $(5MAP)CuCl_3$ salt was not made. If insufficient $CuCl_2$ was added to the final solution, yellow platelets of $(5MAP)_2CuCl_4$ crystallized out as an impurity.[28] Anal. Found (calcd): C, 20.83 (20.81); H, 2.66 (2.62); N, 8.22 (8.09).

Bis(5-bromo-6-methyl-2-aminopyridinium) Octabromotricuprate(II) ($(5B6MAP)_2Cu_3Br_8$, $C_{12}H_{16}N_2Cu_3Br_{10}$). The procedure involved dissolving the 6-methyl-2-aminopyridinium salt and excess $CuBr_2$ in dilute HBr solution. Evaporation of the solution yielded dark purple needlelike crystals of the 5-bromo-6-methyl-2-aminopyridinium salt. Bromination of the pyridine ring (see Structure Descriptions) presumably was catalyzed by the Cu(II) ions.

Methylphenethylammonium Heptachlorotricuprate(II)–Ethanol ($(NMPH)Cu_3Cl_7{\cdot}EtOH$, $C_{11}H_{20}NOCu_3Cl_7$). This salt was prepared by reaction of the amine hydrochloride with excess anhydrous copper(II) chloride in ethanol solution. Initial crystallization yielded red crystals of $(NMPH)_2Cu_2Cl_6$.[29] Upon repeated recrystallization from absolute ethanol, flat orange plates of the heptachloride crystallized.

***N*-Methylpiperazinium Octachlorotricuprate(II) ($(NMPZ)Cu_3Cl_8$, $C_5H_{14}N_2Cu_3Cl_8$).** N-Methylpiperazine dihydrochloride and $CuCl_2{\cdot}2H_2O$ were dissolved in a concentrated HCl solution in a 1:4 ratio. The octachloride salt separated out upon evaporation of the solvent. Anal. Found (calcd): C, 10.87 (10.41); H, 2.43 (2.45); N, 5.11 (4.86).

X-ray Data Collection and Analysis

The X-ray diffraction data collections were carried out on one of three X-ray diffraction systems: a Picker four-circle goniometer automated with a PDP-8L computer[30] ($(3MAP)_2Cu_3Cl_8$), a Nicolet R3m/E diffractometer[31] ($(NMPH)Cu_3Cl_7{\cdot}EtOH$, $(5B6MAP)_2Cu_3Br_8$), or a Philips PW 1100[32] ($(NMPZ)Cu_3Cl_8$). Data collection parameters are listed in Table I. Crystal structure analyses were carried out, respectively, on a locally assembled set of standard programs,[33] the SHELXTL-84 programs from a Nicolet R3m/E system,[34] and the SHELX-76 programs on a CDC Cyber 7600 computer.[35]

Crystal structure solutions were initiated via either direct methods or Patterson techniques. The substituted 2-aminopyridinium salts all grew as fine needles, which were composites of many slightly misoriented crystallites. For the 3MAP salt, the diffraction maxima were broad with a substantial amount of structure. In order to obtain sufficient volume for satisfactory X-ray intensity, long needles had to be selected, and thus the absorption problem was significant. For the 5MAP salt, better crystals were obtained, but the monoclinic crystals were invariably twinned in such a fashion that the $h,k,2l$ and $h,k,\overline{2l+1}$ reflections were superimposed when k was even. Thus, a structure determination was not undertaken. The laminar crystals of $(NMPH)Cu_3Cl_7{\cdot}EtOH$ were com-

(14) Willett, R. D.; Dwiggens, C., Jr.; Kruh, R. F.; Rundle, R. E. *J. Chem. Phys.* **1963**, *38*, 2429.
(15) Roberts, S. A.; Bloomquist, D. R.; Willett, R. D.; Dodgen, H. W. *J. Am. Chem. Soc.* **1981**, *103*, 2603.
(16) Colombo, A.; Menabue, L.; Motori, A.; Pellacani, G. C.; Porzio, W.; Sandrolini, F.; Willett, R. D. *Inorg. Chem.* **1985**, *24*, 2900.
(17) Willett, R. D.; Rundle, R. E. *J. Chem. Phys.* **1964**, *40*, 838.
(18) Swank, D. D.; Willett, R. D. *Inorg. Chim. Acta* **1974**, *8*, 143.
(19) Fletcher, R.; Hansen, J. J.; Livermore, J.; Willett, R. D. *Inorg. Chem.* **1982**, *22*, 2429.
(20) Brown, D. B.; Wasson, J. R.; Hall, J. W.; Hatfield, W. E. *Inorg. Chem.* **1977**, *16*, 2526.
(21) Knuuttila, H. *Inorg. Chem. Acta* **1981**, *50*, 221.
(22) Chiari, B.; Piovesana, O.; Tarantelli, T.; Zanazzi, P. F. *Inorg. Chem.* **1985**, *24*, 4615.
(23) Baker, W. A., Jr.; Helm, F. T. *J. Am. Chem. Soc.* **1975**, *97*, 2295.
(24) Beckett, R.; Colton, R.; Hoskins, B. F.; Martin, R. L.; Vince, D. G. *Aust. J. Chem.* **1969**, *22*, 2527.
(25) Ross, P. F.; Murmann, R. K.; Schlemper, E. O. *Acta Crystallogr., Sect. B: Struct. Crystallogr. Cryst. Chem.* **1974**, *B30*, 1120.
(26) Epstein, J. M.; Figgis, B. N.; White, A. H.; Willis, A. C. *J. Chem. Soc., Dalton Trans.* **1974**, 1954.
(27) Gruber, S. J.; Harris, C. M.; Sinn, E. *J. Chem. Phys.* **1968**, *49*, 2183.
(28) Willett, R. D.; Place, H., submitted for publication in *Acta Crystallogr.*
(29) Harlow, R. L.; Wells, W. J., III; Watt, G. W.; Simonsen, S. H. *Inorg. Chem.* **1974**, *13*, 2860.
(30) Busing, W. R.; Ellison, R. D.; Levy, H. A.; King, S. P.; Roseberry, R. T. "The Oak Ridge Computer-Controlled X-ray Diffractometer"; Report No. ORNL-4143, Oak Ridge National Laboratory: Oak Ridge, TN, 1968.
(31) Campana, C. F.; Shepherd, D. F.; Litchman, W. N. *Inorg. Chem.* **1980**, *20*, 4039.
(32) *Users Manual for PW1100 Philips*; Philips: Eindhoven, The Netherlands.
(33) Caputo, R. Ph.D. Thesis, Washington State University, 1974.
(34) Sheldrick, G. "SHELXTL, Version 4.1"; Nicolet Analytical Instruments: Madison, WI, 1984.
(35) Sheldrick, G. *SHELX-76 Systems of Programs*; University of Cambridge: Cambridge, England, 1976.

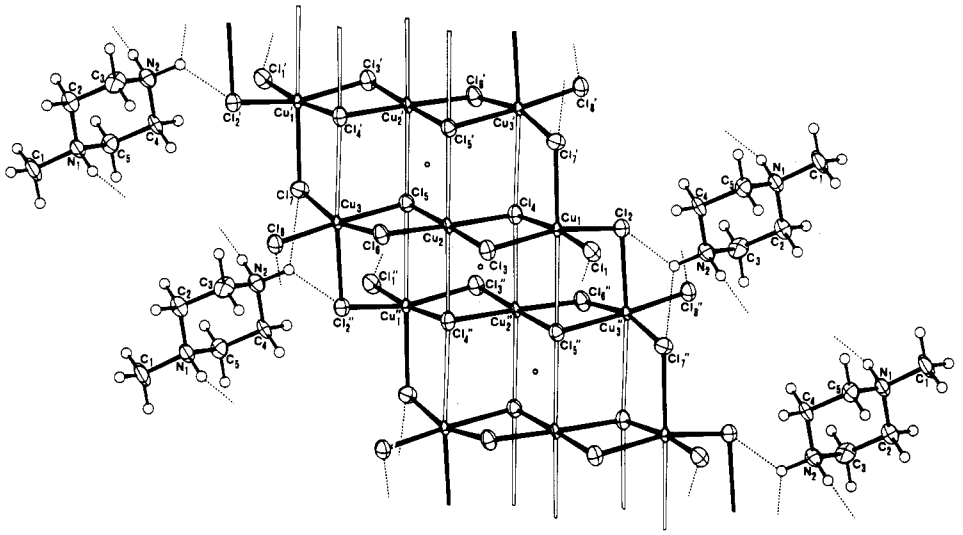

Figure 1. Illustration of stacking of trimers and of hydrogen bonding in $(NMPZ)Cu_3Cl_8$.

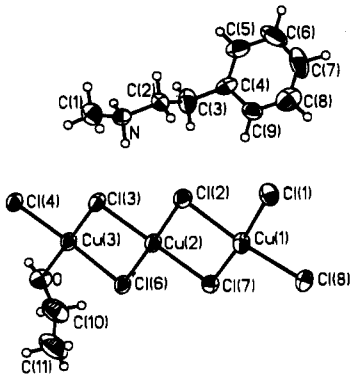

Figure 2. Illustration of the asymmetric unit in $(NMPH)Cu_3Cl_7$·EtOH.

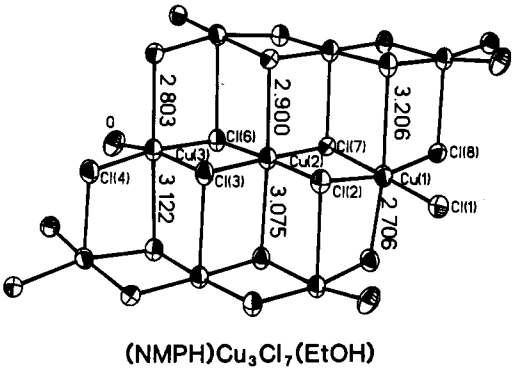

Figure 3. Stacking of trimers in $(NMPH)Cu_3Cl_7$·EtOH.

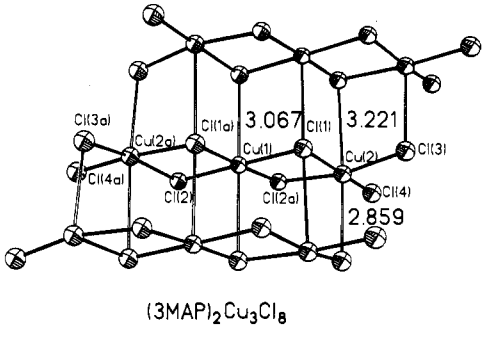

Figure 4. Stacking of trimers in $(3MAP)_2Cu_3Cl_8$.

posites of layers of platelets that also had very poor diffraction characteristics. Refinements generally proceeded smoothly. Difficulty was encountered for $(3MAP)_2Cu_3Cl_8$, in which a substantial disorder problem was found. Approximately 80% of the $Cu_3Cl_8^{2-}$ ions occupied normal sites. The other 20% occupied closely related sites involving overlap of half of the chloride ion positions between the two types of sites. The programs used[32] were not capable of constrained refinement of site occupancy factors. Thus, the 80%–20% split was obtained by trial and error; e.g., it gave better results than 75%–25% and 85%–15% splits. This implies the disorder of the pyridinium cations also. The occupancy of the primary site for the cation was fixed at 80%. It was not possible to resolve the remaining 20% of the cations on the resulting difference Fourier maps. Since their location was not crucial to the interpretation of the magnetic behavior, no attempt was made to pursue the structure refinement. For the NMPZ salt, where twinning of the crystals was also a problem, it was necessary to exclude 43 reflections from the final calculation where F_o was much greater than F_c and where either the scan showed a double peak or the peak was badly miscentered. Refinement of the bromide salt presented a different problem. After the $Cu_3Br_8^{2-}$ ion was located, another substantial peak appeared on the difference electron density map in the area of the pyridinium ring. We had observed structural evidence for the bromination of substituted pyridinium rings previously[36] and thus identified this peak as a bromine atom. Refinement of the occupancy factor indicated 75 (3)% of the pyridinium rings were brominated. Pertinent copper–halide bond distances and angles are given in Table II and Figures 1–5. Final positional parameters are given in Tables III–VI. Tables of hydrogen atom positions, anisotropic thermal parameters, all bond distances and angles, and $|F_o|$ and $|F_c|$ values are deposited as supplementary material, as well as stereographic diagrams.

Structure Descriptions

The crystal structures of these salts all contain pseudoplanar bibridged $Cu_3X_8^{2-}$ or $Cu_3X_7L^-$ anions. Similar neutral $Cu_3Cl_6L_2$ oligomers were found in $Cu_3Cl_6(CH_3CN)_2$[37] and $Cu_3Cl_6(H_2O)_2\cdot2(CH_2)_4SO_2$,[38] and a $Cu_3Br_8^{2-}$ anion was found in $(Et_2NH_2)_2Cu_3Br_8\cdot CuBr_2\cdot EtOH$.[19] Corresponding binuclear, tetranuclear, and pentanuclear oligomers are also known.[9] Within each oligomer, the copper(II) ions attain a square-planar coordination. The Cu–X distances generally range from 2.23 to 2.33 Å for the chloride salts, with the longer distances associated with the bridging halide ions. Bridging angles, important for magnetic–structural correlations, range from 92 to 95°. Intratrimer bond lengths and angles are summarized in Table IIa. Stacking of the trinuclear units, with the formation of long semicoordinate

(36) Place, H. P.; Willett, R. D., submitted for publication in *Acta Crystallogr.*

(37) Willett, R. D.; Rundle, R. E. *J. Chem. Phys.* **1964**, *40*, 838.
(38) Swank, D. D.; Willett, R. D. *Inorg. Chim. Acta* **1978**, *8*, 143.

Table I. X-ray Data Collection Parameters

compd name	*N*-methylpiperazinium octachlorotricuprate(II)	bis(3-methyl-2-amino-pyridinium) octachloro-tricuprate(II)	methylphenethylammonium heptachlorotricuprate(II)–ethanol	bis(5-bromo-6-methyl-2-aminopyridinium) octabromotricuprate(II)
empirical formula	$C_5H_{14}N_2Cu_3Cl_8$	$C_{12}H_{18}N_4Cu_3Cl_8$	$C_{11}H_{20}NOCu_3Cl_7$	$C_{12}H_{10}N_4Cu_3Br_{10}$
mol wt	576.44	692.57	621.09	1204.5
diffractometer syst	Philips PW 1100	Picker	Nicolet R3m/E	Nicolet R3m/E
cryst class	monoclinic	monoclinic	monoclinic	monoclinic
space group	$P2_1/c$	$C2/c$	$P2_1/n$	$P2_1/n$
lattice constants				
a, Å	6.840 (3)	26.05 (1)	11.843 (4)	13.216 (3)
b, Å	14.321 (9)	13.687 (4)	7.626 (3)	4.076 (1)
c, Å	9.890 (5)	7.099 (3)	23.840 (10)	24.61 (6)
β, deg	102.90 (5)	117.95 (3)	79.61 (3)	91.65 (2)
V, Å^3	1604 (1)	2236 (1)	2117 (1)	1325 (1)
no. of reflcns	15	12	25	25
2θ range, deg	$20 < 2\theta < 24$	$38 < 2\theta < 41$	$27 < 2\theta < 31$	$29 < 2\theta < 31$
F(000)	1132	1372	1227.8	1106
radiation	Mo Kα with graphite monochromator	Mo Kα with Zr filter	Mo Kα with Zr filter	Mo Kα with graphite monochromator
cryst size, mm^3	0.29 × 0.39 × 0.78	0.083 × 0.20 × 0.45	0.1 × 0.2 × 0.4	0.14 × 0.06 × 0.02
abs coeff, cm^{-1}	52.88	38.9	38.9	184.5
calcd density, ρ, g cm^{-3}	2.39 (Z = 4)	2.06 (Z = 4)	1.94 (Z = 4)	3.02 (Z = 2)
type of abs cor	numerical	numerical	empirical Ψ scan	numerical
max transmission	1.00	0.83	0.73	0.73
min transmission	0.71	0.73	0.56	0.38
data collecn technique	θ–2θ scan	θ–2θ scan	ω scan	ω scan
scan range, deg	1.8	1.8	2.2	2
scan speed, deg min^{-1}	6.0	8.9	5.86 (min), 29.30 (max)	3.91 (min), 29.30 (max)
check rflcns	$\bar{2}$,12,0	$\bar{1}$5,1,2; $\bar{7}$53; 751	0$\bar{6}\bar{4}$; 0$\bar{6}\bar{2}$; $\bar{2}\bar{3}\bar{1}$	$\bar{1}2\bar{1}$; $\bar{2}\bar{3}0$; $\bar{3}50$
monitoring rate	every 1 h	every 40 rflcns	every 100 rflcns	every 100 rflcns
total rflcns	2943	4401	2323	1316
2θ(max), deg	48	62	40	45
unique rflcns	1966 with $I > 3\sigma(I)$	3754, 1811 with $I > 3\sigma(I)$	1979, 1290 with $F > 3\sigma(F)$	1239, 855 with $F > 3\sigma(F)$
R for equiv rflcns	0.066		0.0406	0.0885
structure solution package	SHELX-76	Washington State University	Nicolet SHELXTL	Nicolet SHELXTL
structure solution technique	Patterson	direct methods	direct methods	direct methods
$R = \sum\|\|F_o\| - \|F_c\|\|/\|F_o\|$	0.043	0.116	0.048	0.058
$R_w = [\sum w(\|F_o\| - \|F_c\|)^2/\sum w\|F_o\|^2]^{1/2}$	0.054	0.120	0.035	0.053
g for $w = 1/[\sigma^2(F) + g(F)^2]$	3×10^{-3}	0	0.000 01	0.000 12
Δ/σ (mean)		0.12	0.11	0.015
Δ/σ (max)		0.45	0.44	0.004
goodness of fit		2.36	1.43	1.575
total params refined	181	117	210	121
thermal params	anisotropic on all non-H atoms	anisotropic on all Cu and Cl atoms	anisotropic on all non-H atoms	anisotropic on all non-H atoms
H atoms	Co–H and N–H fixed at 1.08, thermal params 10% larger than the corresponding heavy atom	omitted	constrained to C–H and N–H = 0.96 Å, thermal params fixed at 0.10	constrained to C–H and N–H = 0.96, thermal params fixed 10% larger than the corresponding heavy atom
largest peak on final diff map, e Å^{-3}	0.4	2.2, near Cl(8)	0.5, near C(1)	1.41, near Cu(1)
extinction cor	no	no	yes	no

Table II. Bond Distances and Angles in $Cu_3X_8^{2-}$ Anions

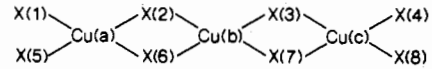

(a) Intratrimer Bond Distances (Å) and Angles (deg)

	Cu(*n*)–X(*n'*)							
	NMPZ		3MAP		NMPH		5B6MAP	
bond	*n*–*n'*	dist	*n*–*n'*	dist	*n*–*n'*	dist	*n*–*n'*	dist
a–1	1–1	2.224 (3)	2–8	2.224 (6)	1–1	2.292 (3)	1–3	2.393 (4)
a–2	1–3	2.311 (3)	2–5	2.296 (5)	1–2	2.319 (3)	1–2	2.448 (5)
a–5	1–2	2.227 (2)	2–6	2.263 (6)	1–8	2.255 (3)	1–4	2.388 (5)
a–6	1–4	2.333 (3)	2–2	2.411 (5)	1–7	2.379 (3)	1–1	2.479 (4)
b–2	2–3	2.235 (3)	1–5	2.251 (6)	2–2	2.274 (3)	2–2	2.389 (3)
b–3	2–6	2.236 (3)			2–3	2.254 (3)		
b–6	2–4	2.257 (2)	1–2	2.326 (5)	2–7	2.273 (3)	2–1	2.425 (3)
b–7	2–5	2.254 (3)			2–6	2.290 (4)		
c–3	3–6	2.319 (3)			3–3	2.288 (3)		
c–4	3–8	2.210 (3)			3–4	2.246 (3)		
c–7	3–5	2.328 (3)			3–6	2.330 (3)		
c–8	3–7	2.232 (3)			3–O	1.968 (8)		
	NMPZ		3MAP		NMPH		5B6MAP	
bond	*n*–*n'*–*n''*	angle	*n*–*n'*–*n''*	angle	*n*–*n'*–*n''*	angle	*n*–*n'*–*n''*	angle
				X(*n*)–Cu(*n'*)–X(*n''*)				
1–a–2	1–1–3	90.7 (1)	8–2–5	91.8 (2)	1–1–2	90.6 (1)	3–1–2	90.5 (2)
1–a–5	1–1–2	94.0 (1)	8–2–6	94.7 (2)	1–1–8	93.8 (1)	3–1–4	93.4 (1)
1–a–6	1–1–4	172.7 (1)	8–2–2	175.5 (2)	1–1–7	174.2 (1)	3–1–1	172.9 (2)
2–a–6	3–1–2	163.2 (1)	5–2–6	167.0 (2)	2–1–8	165.9 (1)	2–1–4	175.2 (2)
2–a–6	3–1–4	83.7 (1)	5–2–2	84.6 (2)	2–1–7	83.9 (1)	2–1–1	84.5 (1)
5–a–6	2–1–4	90.1 (1)	6–2–2	88.2 (2)	8–1–7	91.3 (1)	4–1–1	91.4 (2)
2–b–3	3–2–6	92.3 (1)	5–1–5	94.2 (3)	2–2–3	91.2 (1)	2–2–1′	93.1 (1)
2–b–6	3–2–4	87.3 (1)	5–1–2	87.6 (1)	2–2–7	87.3 (1)	2–2–1	86.9 (1)
2–b–7	3–2–5	178.4 (1)	5–1–2′	177.4 (2)	2–2–6	177.3 (1)	2–2–2′	180
3–b–6	6–2–4	178.0 (1)	2–1–5′	177.4 (2)	3–2–7	178.2 (1)	1′–2–1	180
3–b–7	6–2–5	86.9 (1)			3–2–6	86.9 (1)		
6–b–7	4–2–5	93.6 (1)	2–1–2′	90.6 (3)	7–2–6	94.6 (1)		
3–b–4	6–3–8	90.5 (1)			3–3–4	90.6 (3)		
3–c–7	6–3–5	83.3 (1)			3–3–6	85.2 (1)		
3–c–8	6–3–7	163.1 (1)			3–3–O	169.1 (3)		
4–c–7	8–3–5	173.7 (1)			4–3–6	171.6 (1)		
4–c–8	8–3–7	95.6 (1)			4–3–O	88.9 (2)		
7–c–8	5–3–7	90.6 (1)			7–3–O	93.8 (1)		
				Cu(*n*)–X(*n'*)–Cu(*n''*)				
a–2–b	1–3–2	94.6(1)	2–5–1	96.1 (2)	1–2–2	95.0 (1)	1–2–2	95.1 (1)
a–6–b	1–4–2	93.4 (1)	2–2–1	91.1 (2)	1–7–2	93.4 (1)	1–1–2	93.4 (1)
b–3–c	2–6–3	94.7 (1)			2–3–3	94.9 (1)		
b–7–c	2–5–3	94.0 (1)			2–6–3	92.8 (1)		

(b) Intertrimer Distances (Å)

NMPZ		3MAP		NMPH		5B6MAP	
Cu(1)–Cl(7)	2.655 (3)	Cu(1)–Cl(2)	3.074 (4)	Cu(1)–Cl(4)	2.706 (3)	Cu(2)–Br(1)	3.213 (4)
Cu(1)–Cl(5)	3.240 (3)	Cu(2)–Cl(2)	3.216 (4)	Cu(1)–Cl(6)	3.206 (3)	Cu(1)–Br(2)	3.285 (4)
Cu(2)–Cl(4)	2.979 (3)	Cu(2)–Cl(6)	2.852 (4)	Cu(2)–Cl(3)	3.075 (3)	Cu(1)–Br(4)	3.177 (4)
Cu(2)–Cl(5)	2.972 (3)			Cu(2)–Cl(7)	2.900 (3)		
Cu(3)–Cl(2)	2.667 (3)			Cu(3)–Cl(2)	3.122 (3)		
Cu(3)–Cl(4)	3.226 (3)			Cu(3)–Cl(8)	2.803 (3)		

Cu–X bonds, leads to a final 4+2 coordination for each copper ion, resulting in different possible stacking patterns, as discussed in the abstract and Introduction.

(NMPZ)Cu_3Cl_8. The geometry of the $Cu_3Cl_8^{2-}$ anion in this salt illustrates the characteristics usually associated with pseudoplanar oligomers. Although it lacks any crystallographic symmetry elements, the ion has nearly twofold symmetry. The interior Cl–Cu–Cl angles are systematically less than 90° (85.5° average) while the terminal angles are greater than 90° (94.8° average). Thus the lateral Cl–Cu–Cl angles at the terminal copper atoms are close to 90° (90.5° average) while at the central copper atom they increase to 93.0° (average). The bridging Cu–Cl–Cu angles average 94.2°. Systematic variations are also seen in the bond distances. The terminal Cu–Cl bonds average 2.232 Å while the bridging bonds are longer, averaging 2.270 Å. A substantial trans effect is seen, with the Cu–Cl bonds trans to the terminal Cu–Cl bonds averaging 2.323 Å.

The stacking pattern is of the type IIa, which is a $3(^1/_2, ^1/_2)(^1/_2, -^1/_2)$ pattern in the notation of ref 9. This was the first example found of a trimer with this type of pattern. Each of the three copper atoms complete their coordination sphere by forming two semicoordinate bonds, yielding chains of trimers running parallel to the *a* axis. While the central copper atom, Cu(2), has essentially equal axial bond lengths of 2.975 and 2.979 Å, the situation with the terminal copper atoms is much different. These copper atoms form one semicoordinate bond to a bridging chloride ion and a second to a terminal chloride ion. The latter interaction will clearly be stronger electrostatically, and thus the copper ions and terminal chloride ions are pulled toward each other, forming short semicoordinate bonds of 2.655 Å for Cu(1)–Cl(7′) and 2.667 Å for Cu(3)–Cl(2″). The other semicoordinate bonds are much longer at 3.241 and 3.226 Å, respectively. This distortion from the planarity can be seen in Figure 1. While the coordination at Cu(2) is clearly of the standard 4+2 type, the coordination at

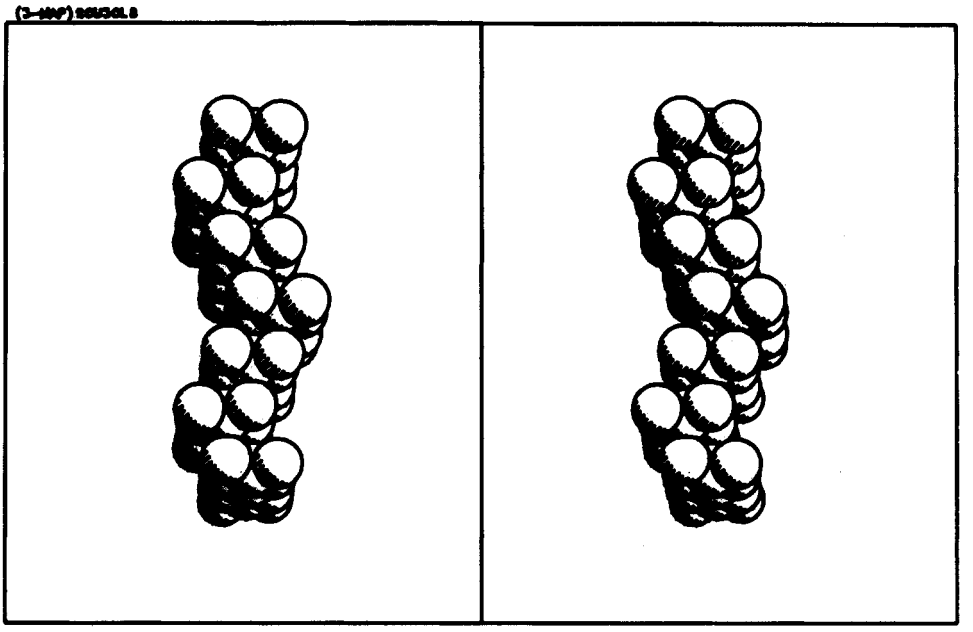

Figure 5. Illustration of disorder in $(3MAP)_2Cu_3Cl_8$.

Table III. Positional ($\times 10^4$) and Isotropic Thermal Parameters ($\times 10^3$) for $(NMPZ)Cu_3Cl_8$[a]

	x	y	z	U, Å²
Cu(1)	732 (2)	37610 (5)	979 (1)	12 (1)
Cu(2)	2781 (2)	50030 (4)	879 (1)	14 (1)
Cu(3)	4871 (2)	62480 (5)	857 (1)	13 (1)
Cl(1)	270 (4)	3236 (1)	2723 (3)	33 (1)
Cl(2)	−1317 (3)	3266 (1)	−633 (2)	25 (1)
Cl(3)	2076 (4)	4451 (1)	2513 (2)	27 (1)
Cl(4)	1081 (3)	4405 (1)	−700 (2)	24 (1)
Cl(5)	3446 (3)	5579 (1)	−746 (2)	24 (1)
Cl(6)	4558 (4)	5575 (1)	2456 (2)	28 (1)
Cl(7)	5856 (4)	6724 (1)	−802 (3)	29 (1)
Cl(8)	6137 (3)	6824 (1)	2555 (3)	28 (1)
C(1)	2139 (20)	−558 (4)	492 (13)	41 (7)
C(2)	4209 (15)	−1421 (4)	575 (10)	31 (5)
C(3)	4158 (15)	−2028 (4)	538 (12)	34 (6)
C(4)	884 (15)	−1992 (4)	−1045 (11)	29 (6)
C(5)	914 (14)	−1385 (4)	−967 (10)	28 (5)
N(1)	2120 (13)	−1187 (3)	371 (9)	26 (5)
N(2)	2911 (12)	−2214 (3)	−813 (9)	31 (5)

[a] The equivalent isotropic U values are defined as one-third of the trace of the orthogonalized U_{ij} tensor.

Cu(1) and Cu(3) might better be labeled as a 4+1+1 coordination. Indeed, around Cu(3), one of the Cl–Cl distances involving the semicoordinate atoms, Cl(8)–Cl(2″), becomes smaller than the sum of the van der Waals radii. A similar coordination behavior is seen in $(melH_2)Cu_2Cl_6$.[16] The net result of this interaction is that the central copper atom retains the planarity of its primary coordination sphere, while the terminal copper atoms have a substantial distortion from planarity (of the "sedia" or "bifold" type[39,40]).

The geometry of the cation is normal, and its packing appears to be largely dictated by hydrogen-bonding constraints. Thus, N(1) (with only one proton) forms a very short hydrogen bond (N–Cl = 3.09 Å) to Cl(1). The latter is one of the terminal chloride ions not involved in a semicoordinate bond. N(2) forms a normal hydrogen bond (N–Cl = 3.16 Å) to the other terminal chloride ion, Cl(8), and a bifurcated hydrogen bond (N–Cl = 3.24 and 3.27 Å) to the two chloride ions Cl(2) and Cl(7), which are involved in semicoordination. This is the behavior anticipated from

(39) O'Brien, S.; Gaura, R. M.; Landee, C. P.; Ramakrishna, B. L.; Willett, R. D., submitted for publication in *Inorg. Chim. Acta*.
(40) Antolini, L.; Manfredini, T.; Pellacani, G. C.; Sandrolini, F.; Motori, A.; Battaglia, L. P.; Bonamartini-Corradi, A.; Geiser, U.; Willett, R. D. *J. Chem. Soc., Dalton Trans.*, in press.

Table IV. Positional ($\times 10^4$) and Isotropic Thermal Parameters ($\times 10^3$) for $(NMPH)Cu_3Cl_7 \cdot EtOH$[a]

	x	y	z	U, Å²
Cu(1)	7156 (1)	4145 (2)	612 (1)	36 (1)
Cu(2)	4988 (2)	2570 (2)	7 (1)	34 (1)
Cu(3)	2889 (1)	694 (2)	−553 (1)	35 (1)
Cl(1)	7609 (2)	3796 (4)	1501 (1)	38 (1)
Cl(2)	5493 (2)	2517 (4)	882 (1)	37 (1)
Cl(3)	3520 (2)	712 (4)	299 (1)	36 (1)
Cl(4)	1554 (3)	−1324 (4)	−219 (1)	39 (1)
O	2554 (7)	310 (10)	−1323 (3)	47 (3)
Cl(6)	4469 (3)	2482 (4)	−873 (1)	36 (1)
Cl(7)	6498 (2)	4405 (4)	−270 (1)	32 (1)
Cl(8)	8468 (3)	6278 (4)	359 (1)	36 (1)
N	370 (7)	3852 (11)	1001 (3)	38 (4)
C(1)	617 (10)	1971 (15)	1079 (5)	52 (5)
C(2)	868 (10)	5034 (15)	1385 (4)	42 (5)
C(3)	513 (11)	6907 (17)	1355 (5)	63 (6)
C(4)	1018 (9)	8131 (16)	1747 (5)	41 (5)
C(5)	455 (11)	8641 (17)	2284 (5)	61 (6)
C(6)	953 (14)	9712 (18)	2618 (5)	90 (8)
C(7)	2048 (15)	10283 (19)	2402 (6)	86 (8)
C(8)	2623 (11)	9764 (17)	1895 (5)	68 (6)
C(9)	2140 (10)	8682 (15)	1567 (5)	49 (5)
C(10)	2847 (11)	1348 (20)	−1840 (6)	76 (7)
C(11)	3861 (12)	808 (20)	−2171 (6)	108 (8)

[a] See footnote *a* of Table III.

Table V. Positional ($\times 10^4$) and Isotropic Thermal Parameters ($\times 10^3$) for $(5B6MAP)_2Cu_3Br_8$[a]

	x	y	z	U, Å²
Cu(2)	5000	5000	0	35 (2)
Cu(1)	5223 (3)	1320 (10)	1314 (1)	36 (1)
Br(1)	6184 (2)	1337 (8)	464 (1)	34 (1)
Br(2)	4039 (2)	4876 (8)	807 (1)	36 (1)
Br(3)	4112 (2)	1203 (8)	2065 (1)	37 (1)
Br(4)	6409 (2)	−2359 (8)	1738 (1)	41 (1)
Br(5)	1378 (4)	8997 (15)	494 (2)	78 (3)
N(1)	99 (17)	4926 (49)	1808 (8)	34 (9)
C(2)	−834 (20)	3775 (69)	1649 (10)	31 (7)
C(3)	−1227 (20)	4615 (97)	1123 (11)	68 (15)
C(4)	−501 (23)	6068 (76)	814 (1)	52 (13)
C(5)	463 (20)	7098 (69)	961 (9)	36 (11)
C(6)	782 (21)	6337 (69)	1476 (10)	34 (8)
N(2)	−1346 (18)	2185 (69)	2024 (9)	70 (12)
C(7)	1787 (19)	6961 (88)	1714 (10)	62 (14)

[a] See footnote *a* of Table III.

Table VI. Positional and Equivalent Isotropic Thermal Parameters for $(3MAP)_2Cu_3Cl_8$[a]

	x	y	z	U, Å²
Cu(1)	0.5	0.4403 (2)	0.25	0.076 (3)
Cu(2)	0.63020 (7)	0.4373 (2)	0.2529 (3)	0.106 (2)
Cl(2)	0.5622 (1)	0.5599 (3)	0.2401 (6)	0.113 (3)
Cl(5)	0.4397 (2)	0.3284 (3)	0.2714 (8)	0.092 (3)
Cl(6)	0.6826 (1)	0.5580 (4)	0.2070 (6)	0.144 (3)
Cl(8)	0.6871 (2)	0.3175 (5)	0.2466 (8)	0.146 (9)
Cu(1′)	0.5	0.6930 (1)	0.25	0.161 (13)
Cu(2′)	0.6315 (4)	0.6830 (8)	0.266 (2)	0.155 (9)
Cl(5′)	0.582 (3)	0.806 (3)	0.242 (9)	0.59 (10)
Cl(8′)	0.692 (2)	0.801 (3)	0.275 (4)	0.18 (3)
N(1)	0.0667 (9)	0.311 (2)	0.225 (3)	0.11 (1)
C(2)	0.1990 (12)	0.308 (2)	0.330 (4)	0.12 (2)
C(3)	0.1723 (8)	0.392 (2)	0.283 (3)	0.18 (1)
C(4)	0.3762 (8)	0.075 (2)	0.247 (3)	0.20 (1)
C(5)	0.3173 (6)	0.072 (1)	0.209 (2)	0.11 (1)
N(6)	0.0899 (7)	0.497 (1)	0.231 (3)	0.16 (1)
C(7)	0.2002 (6)	0.472 (1)	0.303 (2)	0.13 (1)
C(8)	0.1103 (7)	0.401 (1)	0.242 (3)	0.16 (1)

[a] See footnote *a* of Table III.

electroneutrality arguments.[8] Cl(4) and Cl(5) are involved in two normal and two semicoordinate bonds. Cl(3) and Cl(6) form two normal bonds each, while Cl(2) and Cl(7) are each involved in one normal bond, one short semicoordinate bond, and one bifurcated hydrogen bond. Finally, Cl(1) and Cl(8) each form one normal copper–chloride bond and one short hydrogen bond.

$(NMPH)Cu_3Cl_7 \cdot EtOH$. The $Cu_3Cl_7 \cdot EtOH^-$ anion with its corresponding counterion is illustrated in Figure 2. The intraoligomer Cu–Cl distances range from 2.246 to 2.379 Å, with bridging Cu–Cl–Cu angles ranging from 92.8 to 95.0°. Trends in distances and angles are similar to those in $(NMPZ)Cu_3Cl_8$. The ethanol molecule coordinates to one of the terminal copper(II) ions in the trimer (Cu(3)–O = 1.968 Å) with the ethyl group lying out of the plane of the oligomer. This $Cu_nX_{2n+1}L^-$ anion is unique among oligomeric species found to date in copper(II) halide systems. Adjacent oligomers, related by centers of inversion in the monoclinic space group, stack as shown in Figure 3. This is a variation of the $3(^1/_2,^1/_2)$ stacking depicted in IIb. Intertrimer distances range from 2.706 to 3.206 Å.

$(3MAP)_2Cu_3Cl_8$. The $Cu_3Cl_8^{2-}$ ion in this molecule has C_2 symmetry, with Cu–Cl distances within the trimer ranging from 2.224 to 2.326 Å, while intertrimer distances range from 2.952 to 3.216 Å (Figure 4). The stacking is of the type IIa also, as in the NMPZ salt, but with the addition of twofold symmetry operations relating adjacent trimers. Distortions of the trimer are similar in nature to those in the NMPZ salt. As indicated in the previous section, this compound exhibits a severe disorder problem, the nature of which is illustrated in Figure 5. About 20% of the trimers are subject to a stacking fault of the type shown by the middle trimer in Figure 5. That is, instead of alternate stacking in the sequence $(^1/_2,^1/_2)(^1/_2,^{-1}/_2)$..., two successive $(^1/_2,^1/_2)$ steps occur, followed by two successive $(^1/_2,^{-1}/_2)$ steps.

$(5B6MAP)_2Cu_3Br_8$. The structure consists of discrete 5-bromo-6-methyl-2-aminopyridinium cations and $Cu_3Br_8^{2-}$ anions. The bond angles and distances within the cation are normal. The bromination of substituted pyridinium rings has been described elsewhere.[28] The anion is a trimeric species, the copper(II) ions being bibridged through bromide ions. The Cu(2) atom is on a center of inversion and has very nearly square-planar geometry. The geometry at the Cu(1) atom is more distorted from square-planar coordination, both in distances and in angles. The bifold distortion of the terminal copper atoms is not nearly as pronounced in this salt as in the chloride salts.

The trimeric anions stack with a $3(^1/_2,^1/_2)$ pattern such that each copper assumes a 4+2 coordination (Figure 6). The equatorial Cu–Br distances are 2.407 Å (average); the semicoordinate Cu–Br distances range from 3.177 to 3.285 Å. There is hydrogen bonding between the nitrogen in the ring, N(1), and Br(3) (N–Br = 3.31 Å) and between the amino nitrogen, N(2), and Br(4) (N–Br = 3.55 Å). Again, the hydrogen bonding is to the terminal, nonbridging, halide ions.

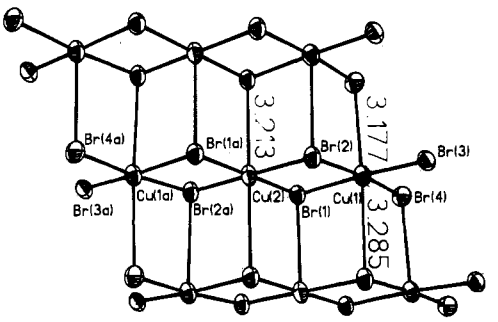

$(5B6MAP)_2Cu_3Br_8$

Figure 6. Stacking of trimers in $(5B6MAP)_2Cu_3Br_8$.

$(5MAP)_2Cu_3Cl_8$. As indicated above, crystals of this salt were invariably twinned. However, it was possible to identify a primitive unit cell with lattice constants of approximately 3.9 Å × 23.6 Å × 24.1 Å and β = 94.6° with a unit cell volume of ~2220 Å³. However, this unit cell arises from two overlapping reciprocal lattices due to the apparent intrinsic twinning in this system. The 3.9-Å *a*-axis lattice constant does dictate a $3(^1/_2,^1/_2)$ stacking pattern (type IIb). Thus each Cu ion assumes a 4+2 coordination geometry.

Magnetic Properties

Within a linear Cu(II) trinuclear oligomer, the magnetic interactions can be modeled quite well by the spin Hamiltonian

$$\mathcal{H} = -2J(\vec{S}_1 \cdot \vec{S}_2 + \vec{S}_2 \cdot \vec{S}_3) \quad (1)$$

which assumes an isotropic exchange interaction and neglects next-nearest-neighbor intratrimer coupling between the end atoms; e.g., $J_{13} = 0$. The energy levels of this Hamiltonian can easily be shown to be $E_1 = 2J$ ($S = ^1/_2$), $E_2 = 0$ ($S = ^1/_2$), and $E_3 = -J$ ($S = ^3/_2$).[41] Thus, the magnetic susceptibility (obtained from the Van Vleck equation) is given by

$$\chi_M = N_1\chi_{1/2} + N_2\chi_{1/2} + N_3\chi_{3/2} \quad (2a)$$

$$\chi_M = \left(\frac{C}{T}\right)\frac{1 + \exp(J/kT) + 10\exp(-3J/kT)}{1 + \exp(J/kT) + 2\exp(-3J/kT)} \quad (2b)$$

where $C = Ng^2\mu_B^2/4k$ and the N_i values are the Boltzmann populations of the *i*th energy levels. Since the trimers stack in a one-dimensional array, it is reasonable to assume it may be necessary to include interoligomer interactions. If these interactions, denoted generically by J', are much less than J, it is traditional to include this as a mean field correction

$$\chi_{M,mf} = \chi_M\left(\frac{T}{T - \theta}\right) \quad (3)$$

with $\theta = ZJ'/k$[42] and where Z is the number of J' exchange pathways. However, for the trimer stacks, this simple argument may not be appropriate if the ground state is antiferromagnetic due to spin frustration effects.

In Figure 7, the exchange pathways of the trinuclear oligomers for $3(^1/_2,^1/_2)$ or $3(^1/_2,^1/_2)(^1/_2,^{-1}/_2)$ patterns are depicted schematically. Labeling of the interoligomer exchange pathways are indicated, along with a possible arrangement of antiferromagnetically coupled trimers. Five pathways are identified: $J_{11'}$, $J_{21'}$, $J_{22'}$, $J_{32'}$, and $J_{33'}$. If these pathways all have the same sign, it can be argued that a "frustration" occurs; e.g., if J_{11} favors a spin-up configuration at site 1′, then $J_{12'}$ favors a spin-down configuration. Similar arguments hold at site 2′. Hence, no net coupling of sites 1′ and 2′ to sites 1, 2, and 3 will occur. Similar arguments hold if the primed copper(II) ions are coupled ferromagnetically ($S = ^3/_2$, quartet state). But, if adjacent oligomers are both in the quartet state, then $J_{11'}$ and $J_{21'}$ reinforce the spin

(41) Gotham, R. W.; Kettle, S. F. A.; Marks, J. A. *J. Chem. Soc., Faraday Trans. 2* **1976**, 125.
(42) Ginsberg, A. P. *Inorg. Chim. Acta, Rev.* **1971**, *5*, 45.

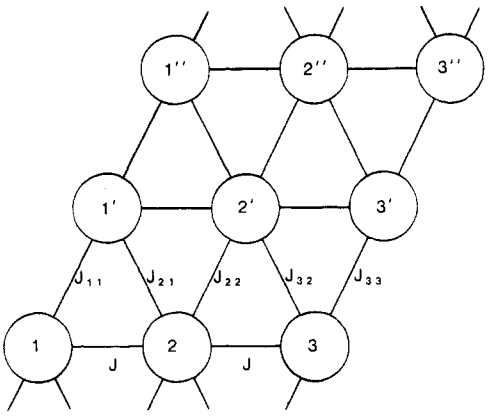

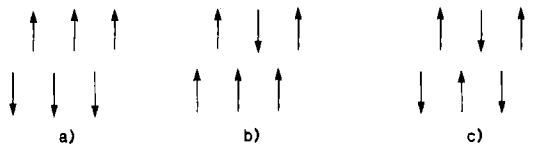

Figure 7. (Top) Spin interaction pathways for the $3(^1/_2,^1/_2)$ and $3(^1/_2,^1/_2)(^1/_2,^{-1}/_2)$ stacking patterns. (Bottom) Spin arrangements for (a) two quartet states, (b) a quartet and a doublet state, and (c) two quartet states.

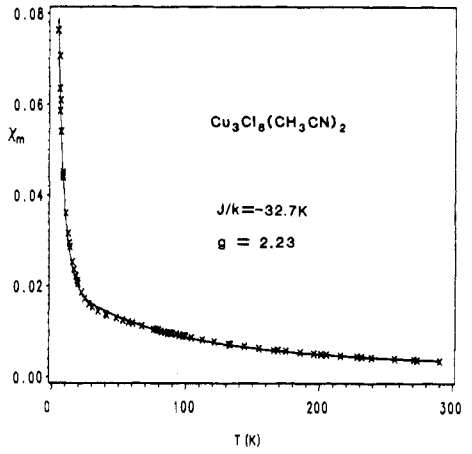

Figure 8. Plot of χ_M vs. T for $Cu_3Cl_6(CH_3CN)_2$. The solid line is the fit to the isolated trimer model with J/k = 32.7 K.

orientation at 1'. Thus, if all J_{ij} values have the same sign, the doublet states are essentially decoupled from the other states. However, coupling will occur between adjacent quartet states. Phenomenologically, this can be modeled by introducing a mean field correction, θ', to the susceptibility of the quartet term in eq 2a to yield

$$\chi_M' = N_1\chi_{1/2} + N_2\chi_{1/2} + N_3\chi_{3/2}\left(\frac{T}{T+\theta'}\right) \qquad (4)$$

Qualitatively, if θ' is negative, this interaction will tend to stabilize the quartet state and add a cooperative flavor to the interaction; e.g., the system will not obey simple Boltzmann statistics.

This cooperativity exhibits itself in several ways in the susceptibility data. Figure 8 shows the χ_M vs. T data for $Cu_3Cl_6(CH_3CN)_2$, a $3(^3/_2,^1/_2)$ structure, which will not be expected to exhibit this phenomenon of spin frustration to a large extent. In the temperature region where depopulation of the quartet state occurs, 30–100 K, χ_M increases steadily and never reaches a maximum. The isolated trimer model (eq 2b) reproduces the data very nicely in this region. In contrast, the χ_M vs. T plot for

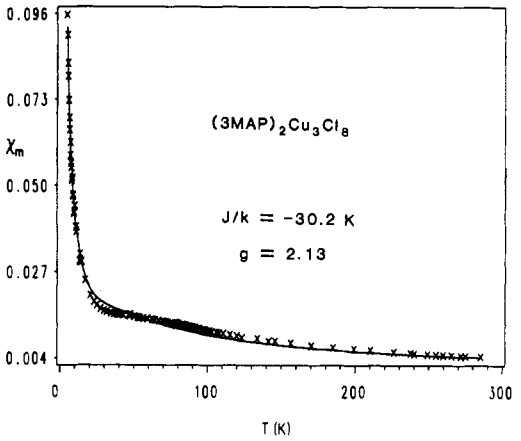

Figure 9. Plot of χ_M vs. T for $(3MAP)_2Cu_3Cl_8$. The solid line is the fit to the isolated trimer model with J/k = −30.2 (8) K.

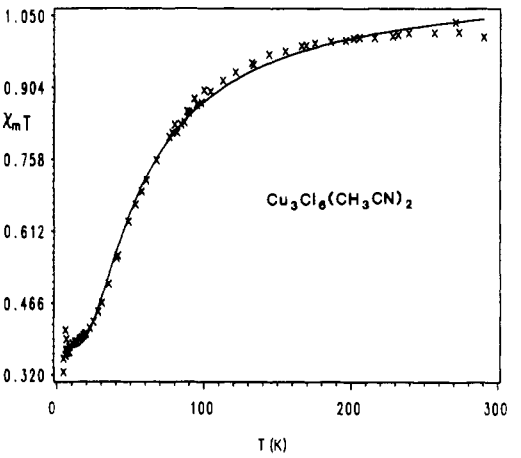

Figure 10. Plot of χ_MT vs. T for $Cu_3Cl_6(CH_3CN)_2$. The solid line is the fit to the isolated trimer model with J/k = 32.7 K.

$(3MAP)_2Cu_3Cl_8$ exhibits a definite flattening in the 30–60 K range (Figure 9). This cannot be reproduced by eq 2b. A related phenomenon occurs in the χ_MT vs. T plots. Figure 10, for $Cu_3Cl_6(CH_3CN)_2$, shows a generally satisfactory agreement between eq 2b and the data. Some small systematic deviations are seen, with the model being too large in the 30–60 K region, too low from 90 to 170 K, and too large again from 220 to 300 K. Some improvement in the lowest temperature range (4–20 K) is obtained by the simple mean field correction (eq 3), as might be anticipated since interstack interactions are possible in this structure. Conversely, the χ_MT vs. T data for $(3MAP)_2Cu_3Cl_8$ (Figure 11) shows serious deviations from eq 2b. At high temperatures, χ_MT is much flatter (constant) than the model, and for intermediate temperatures, χ_MT drops too rapidly. This is indicative of a more cooperative type of behavior. The phenomenological model given in eq 4, however, reproduces the data quite well (solid line in Figure 11). Similar results are seen for the other chloride salts (Figures 12–14 and Table VII), although the magnitude of the mean field correction is smaller, except for the $(5MAP)_2Cu_3Cl_8$ data (Figure 14), which are best fit to the mean field model with θ positive.

Magnetic–Structural Correlations

The first impulse is to compare the J/k values in these planar trimers with those found in the corresponding planar $Cu_2Cl_6^{2-}$ dimers[12] and be gratified with the good agreement. For $KCuCl_3$ and $(melH_2)Cu_2Cl_6$, J/k values of −28 K are obtained.[16] In the trimers whose structures have been determined, the observed values range from −19 to −33 K. However, for planar bibridged copper(II) species, a major correlation between structure and magnetic exchange coupling has been found with the bridging angle, ϕ. In the trimer, the bridging angles are typically 94.0 ± 1.0°, while in the dimers, ϕ = 95.5°. Thus, the trimers should reasonably

Table VII. Comparison of Structural Parameters for Chloride Trimers

	3MAP	CH_3CN	$(CH_2)_4SO_2$	NMPH	NMPZ	5MAP
Cu–Cl(br), Å	2.317	2.288	2.291	2.301	2.370	
Cu–Cl(t), Å	2.248	2.256	2.239	2.260	2.232	
Cu–Cl–Cu, deg	93.6	94.0	93.6	94.1	94.2	
Cu–Cu, Å	3.382	3.346	3.331	3.366	3.456	
Cu–Cl(semicoord), Å						
min	2.859	2.714	2.996	2.706	2.655	
max	3.221	3.185	3.140	3.206	3.266	
Cu–O, Å			1.973	1.968		
Cu–N, Å		1.973				
stacking pattern	$3(^1/_2,^1/_2)(^1/_2,-^1/_2)$	$3(^3/_2,^1/_2)$	$3(^3/_2,^1/_2)$	$3(^1/_2,^1/_2)$	$3(^1/_2,^1/_2)(^1/_2,-^1/_2)$	$3(^1/_2,^1/_2)$
J/k, K	−29.7	−32.7	−21	−19.4	−29.4	−38.2
θ, K	−7.5	−0.7		−4.9	−1.7	+5.0

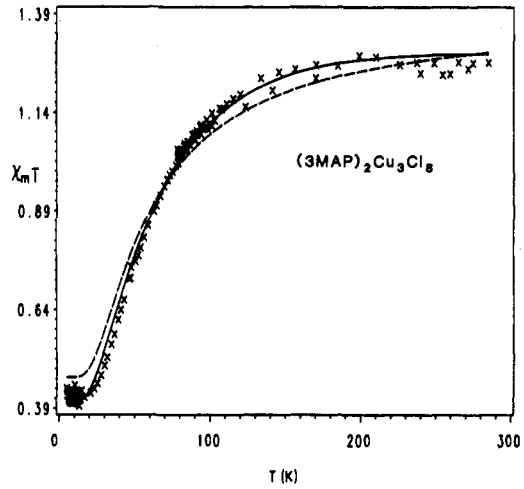

Figure 11. Plot of $\chi_M T$ vs. T for $(3MAP)_2Cu_3Cl_8$. The dashed line is for the isolated trimer model while the solid line is for the mean field corrected model (see text) with J/k = −29.7 K and θ = −7.5 K.

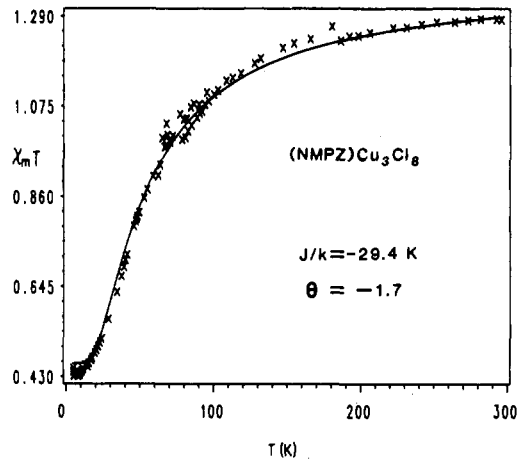

Figure 12. Plot of $\chi_M T$ vs. T for $(NMPZ)Cu_3Cl_8$. The solid line is the fit with J/k = −29.4 K and θ = −1.7 K.

be expected to be less antiferromagnetic. In addition, the terminal copper(II) atoms in the trimer show some significant distortions from planarity. This again should lead to weaker antiferromagnetic behavior,[12,39] in contrast to the observation.

These facts become even more distressing when the results on tetrameric $Cu_4Cl_{10}^{2-}$ ions[43] and the infinite chains in $CuCl_2$ are taken into account. In the tetramer, ϕ again is ~94°, but now $J/k \approx -60$ K. For $CuCl_2$, ϕ is not known, but J/k = −54 K.[44] Similarly, the J/k and ϕ values show the same trend for the bromide series: dimers, J/k = −95 K and $\phi \approx 95.5°$;[45] trimers,

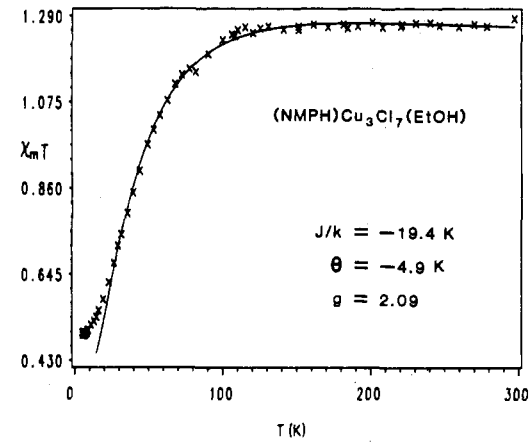

Figure 13. Plot of $\chi_M T$ vs. T for $(NMPH)Cu_3Cl_7$·EtOH. The solid line is the fit with J/k = −19.4 K and θ = −4.9 K.

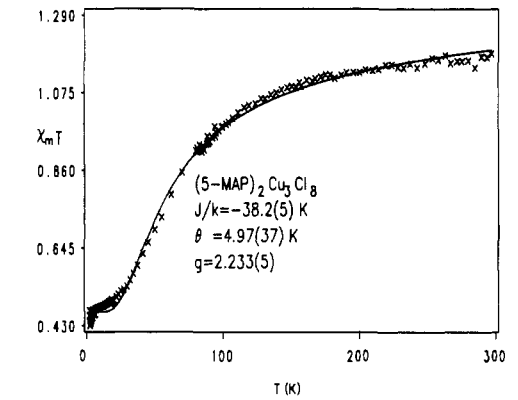

Figure 14. Plot of $\chi_M T$ vs. T for $(5MAP)_2Cu_3Cl_8$. The solid line is the fit with J/k = −38.2 K and θ = 5.0 K.

J/k = −100 K and $\phi \approx 94°$;[19] tetramers, J/k = −180 K and $\phi \approx 94°$;[9] infinite chain, J/k = −165 K and $\phi \approx 92°$.[44] Thus, we are forced to conclude that the degree of polymerization causes a change in the magnitude of the exchange coupling. At this point, its source is not readily apparent.

Acknowledgment. The support of NSF Grants DMR 8219430 and INT-8219425 is acknowledged. The WSU X-ray diffraction laboratory was established through funds from NSF Grant CHE-8408407 and The Boeing Corp.

Supplementary Material Available: Listings of positional coordinates, thermal parameters, and bond distances and angles for $(NMPZ)Cu_3Cl_8$ (Tables 1s–3s), positional coordinates, thermal parameters, and bond distances and angles for $(NMPH)Cu_3Cl_7$·EtOH (Tables 5s–7s), thermal parameters and bond distances and angles for $(3MAP)_2Cu_3Cl_8$ (Tables 9s and 10s), and positional coordinates, thermal parameters, and bond distances and angles for $(5B6MAP)_2Cu_3Cl_8$ (Tables 12s–14s) and stereographic packing diagrams of $(3MAP)_2Cu_3Cl_8$, $(NMPH)Cu_3Cl_7$·EtOH, and $(5B6MAP)_2Cu_3Br_8$ (Figures 15s–17s) (14 pages); listings of observed and calculated structure factors for the four compounds (Tables 4s, 8s, 11s, and 15s) (53 pages). Ordering information is given on any current masthead page.

(43) Halvorson, K.; Grigereit, T.; Willett, R. D. *Inorg. Chem.*, in press.
(44) Willett, R. D. *Inorg. Chem.* **1986**, *25*, 1918. Halvorson, K., private communication.
(45) Inoue, M.; Kishita, M.; Kubo, M. *Inorg. Chem.* **1967**, *6*, 900.